

Coligand-Dependent Shifts in Charge Distribution for Copper Complexes Containing 3,5-Di-*tert*-butylcatecholate and 3,5-Di-*tert*-butylsemiquinonate Ligands

Gabor Speier,^{1a} Sandor Tisza,^{1b} Zoltan Tyeklar,^{1a} Christopher W. Lange,^{1c} and Cortlandt G. Pierpont^{1c}

Department of Chemistry and Biochemistry, University of Colorado, Boulder, Colorado 80309, Department of Organic Chemistry, University of Veszprem, 8201 Veszprem, Hungary, and Research Group for Petrochemistry, Hungarian Academy of Sciences, 8201 Veszprem, Hungary

Received September 1, 1993^o

Cu(py)₂(3,5-DBCat) has been prepared by reacting copper metal with 3,5-di-*tert*-butyl-1,2-benzoquinone (3,5-DBBQ) in pyridine solution. Crystallographic characterization of the complex obtained as the pyridine solvate (triclinic, *P*1, *a* = 13.909(2) Å, *b* = 14.187(2) Å, *c* = 14.570(3) Å, α = 75.26(1)°, β = 72.37(1)°, γ = 80.57(1)°, *V* = 2637.9(9) Å³, *Z* = 2) has shown that the molecule is dimeric with square pyramidal metal ions bridged at basal positions by oxygen atoms of the catecholate ligands. Pyridine ligands occupy basal and apical sites of the centrosymmetric dimer. The magnetic moment for the dimer decreases from 2.84 μ_B at room temperature to 0.52 μ_B at 5.0 K; exchange coupling is antiferromagnetic and has been theoretically fit with a *J* value of -95.3 cm⁻¹. Cu(PPh₃)₂(3,5-DBSQ) has been prepared by reacting stoichiometric proportions of 3,5-DBBQ, PPh₃, and copper metal in acetonitrile solution. When the reaction was carried out with twice the stoichiometric quantity of copper metal, the product obtained was [Cu^I(NCCH₃)(PPh₃)₂][Cu^{II}(3,5-DBCat)₂]. Crystallographic characterization (monoclinic, *P*2₁/*n*, *a* = 16.163(2) Å, *b* = 9.245(1) Å, *c* = 21.312(3) Å, β = 99.78(2)°, *V* = 3138.3(7) Å³, *Z* = 2) has shown that the centrosymmetric complex molecule consists of a central [Cu(3,5-DBCat)₂]²⁻ anion with cationic [Cu(NCCH₃)(PPh₃)₂]⁺ units bonded to bridging oxygen atoms of the catecholate ligands. The EPR spectrum of the complex in the solid state is typical of Cu(II). The EPR spectrum of [Cu^I(NCCH₃)(PPh₃)₂][Cu^{II}(3,5-DBCat)₂] in toluene solution was characteristically the radical spectrum of (PPh₃)₂Cu(3,5-DBSQ). This observation is explained in terms of a Cat-to-Cu(II) electron-transfer reaction.

Introduction

Complexes of copper-containing catechol and semiquinone ligands have been of interest as compounds that combine the redox activity of a transition metal ion with that of an electroactive organic ligand. Both the metal and the ligand may contribute to dioxygen binding and activation in oxidation reactions.² Biological oxidation of a bound catecholate to benzoquinone is thought to occur in the mechanism of tyrosine oxidation by tyrosinase as oxidized Cu(II) centers at the bimetallic site are reduced to the active Cu(I) form.³ A trihydroxyphenylalanine (topa) cofactor operates in conjunction with the metal ion in, at least, one of the copper-containing amine oxidase enzymes, bovine serum amine oxidase.⁴ Growing spectroscopic evidence points to the coordination of a quinoid partially-reduced pterin cofactor with the copper center at the active site of *Chromobacterium violaceum* phenylalanine hydroxylase.⁵ Synthetic catechol oxidation reactions have been studied that lead either to benzoquinone products,⁶ in the manner of tyrosinase, or to ring-opened products of the type associated with the model studies on catechol dioxygenase enzymes.⁷

A common feature of the synthetic and biological copper complexes containing quinone and quinoid ligands is electron

transfer to the metal in steps that either initiate a catalytic cycle or restore a resting condition. As a consequence, electron transfer within the copper-quinone chelate ring has been a point of specific interest in characterization of catecholate and semiquinonate complexes. As a general result, it has been found that ligands which stabilize Cu(I) lead to a Cu^I(SQ) charge distribution, while hard-donor ligands that raise orbital energy on the metal lead to complexes with the Cu^{II}(Cat) charge distribution.⁸ Nitrogen-donor ligands are of the latter type, and the Cu(N-N)(3,5-DBCat) (N-N = bpy, phen) complexes reported by Brown were among the earliest examples of synthetic coordination complexes observed to react with molecular oxygen to give ring-opened oxidation products.^{7a} Subsequent characterizations of these and related complexes of copper have shown that they are often not simple monomeric molecules. Structural studies of Cu(bpy)(3,5-DBCat) have shown that it may exist as either a monomer or a dimer,⁸ and Cu(py)(3,5-DBCat) is tetrameric.⁹ In this report, we describe the properties of Cu^{II}(py)₂(3,5-DBCat), obtained from the reaction between 3,5-di-*tert*-butyl-1,2-benzoquinone (3,5-DBBQ) and copper metal, and characterization of the products obtained from related reactions carried out in the presence of PPh₃.

Experimental Section

Reagent grade chemicals were used in all experiments, and solvents were purified by using standard procedures.

- ^o Abstract published in *Advance ACS Abstracts*, April 1, 1994.
- (a) University of Veszprem. (b) Hungarian Academy of Sciences. (c) University of Colorado.
 - Speier, G.; Tyeklar, Z.; Szabo, L., II; Toth, P.; Pierpont, C. G.; Hendrickson, D. N. In *The Activation of Dioxygen and Homogeneous Catalytic Oxidations*; Barton, H. D., Martell, A. E., Sawyer, D. T., Eds.; Chapman & Hill: New York, 1993.
 - Winkler, M.; Lerch, K.; Solomon, E. I. *J. Am. Chem. Soc.* **1981**, *103*, 7001.
 - Janes, S. M.; Mu, D.; Wemmer, D.; Smith, A. J.; Kaur, S.; Maltby, D.; Burlingame, A. L.; Klinman, J. P. *Science* **1990**, *248*, 981.
 - (a) Pember, S. O.; Benkovic, S. J.; Villafranca, J. J.; Pasenkiewicz-Gierula, M.; Antholine, W. E. *Biochemistry* **1987**, *26*, 4477. (b) Pember, S. O.; Johnson, K. A.; Villafranca, J. J.; Benkovic, S. J. *Biochemistry* **1989**, *28*, 2124.
 - Balla, J.; Kiss, T.; Jameson, R. F. *Inorg. Chem.* **1992**, *31*, 58.

- (a) Brown, D. G.; Beckmann, L.; Ashby, C. H.; Vogel, G. C.; Reinprecht, J. T. *Tetrahedron Lett.* **1977**, 1363. (b) Rojic, M. M.; Swerdloff, M. D.; Demmin, T. R. In *Copper Coordination Chemistry*; Karlin, K. D., Zubieta, J., Eds.; Biochemical and Inorganic Perspectives; Adenine: Guilderland, NY, 1983; p 259.
- Buchanan, R. M.; Wilson-Blumenberg, C.; Trapp, C.; Larsen, S. K.; Greene, D. L.; Pierpont, C. G. *Inorg. Chem.* **1986**, *25*, 3070.
- (a) Olmstead, M. M.; Power, P. P.; Speier, G.; Tyeklar, Z. *Polyhedron* **1988**, *7*, 609. (b) SaF'yanov, Y. N.; Zakharov, L. N.; Struchkov, Y. T.; Lobanov, A. V.; Cherkasov, V. K.; Abakumov, G. A. *Koord. Khim.* **1989**, *15*, 1233.

Table 1. Crystallographic Data for $[\text{Cu}(\text{py})_2(3,5\text{-DBCat})]_2$ and $[\text{Cu}(\text{NCCH}_3)(\text{PPh}_3)]_2[\text{Cu}(3,5\text{-DBCat})_2]$

	$[\text{Cu}(\text{py})_2(3,5\text{-DBCat})]_2^a$	$[\text{Cu}(\text{NCCH}_3)(\text{PPh}_3)]_2[\text{Cu}(3,5\text{-DBCat})_2]^b$
fw	923.6 ^c	1237.8
color	green-brown	brown
crystal system	triclinic	monoclinic
space group	$P\bar{1}$	$P2_1/n$
<i>a</i> , Å	13.909(2)	16.163(2)
<i>b</i> , Å	14.187(2)	9.245(1)
<i>c</i> , Å	14.570(3)	21.312(3)
α , deg	75.26(1)	90.00
β , deg	72.37(1)	99.78(2)
γ , deg	80.57(1)	90.00
<i>V</i> , Å ³	2637.9(9)	3138.3(7)
<i>Z</i>	2	2
<i>D</i> _{calcd} , g cm ⁻³	1.193	1.304
μ , mm ⁻¹	1.308	1.106
<i>R</i> , <i>R</i> _w ^d	0.053, 0.065	0.037, 0.056
GOF	1.13	1.38

^a Radiation Cu K α (λ 1.541 84 Å); temperature 295–297 K. ^b Radiation Mo K α (λ 0.710 73 Å); temperature 295–298 K. ^c For formula $[\text{Cu}(\text{py})_2(3,5\text{-DBCat})]_2 \cdot 0.5\text{C}_5\text{H}_5\text{N}$. ^d $R = \sum ||F_o| - |F_c|| / \sum |F_o|$; $R_w = [\sum w(|F_o| - |F_c|)^2 / \sum w(F_o)^2]^{1/2}$.

$[\text{Cu}(\text{py})_2(3,5\text{-DBCat})]_2$. A mixture of 3,5-DBBQ (2.2 g, 10 mmol) and copper powder (1.27 g, 20 mmol) in pyridine (35 mL) was refluxed under argon for 3 h. Unreacted copper was removed by filtration, the filtrate was reduced in volume under vacuum, and ether (10 mL) was added. The product was obtained as brown crystals (3.2 g, 76% yield) that were found to form as a pyridine solvate, $[\text{Cu}(\text{py})_2(3,5\text{-DBCat})]_2 \cdot 0.5\text{C}_5\text{H}_5\text{N}$. IR (Nujol): 1464, 1259 cm⁻¹. UV-vis [CH_2Cl_2 ; cm⁻¹ (log ϵ ; ϵ units M⁻¹ cm⁻¹): 39 400 (4.46), 38 550 (4.52), 37 800 (4.52) 36 900 (4.44), 24 000 (3.77). Anal. Calcd for $\text{C}_{50.5}\text{H}_{62.5}\text{H}_4.5\text{O}_4\text{Cu}_2$: C, 65.67; H, 6.82; N, 6.82. Found: C, 63.83; H, 6.51; N, 6.17.

$\text{Cu}(\text{PPh}_3)_2(3,5\text{-DBSQ})$. 3,5-DBBQ (1.1 g, 5.0 mmol) and PPh_3 (2.63 g, 10 mmol) were dissolved in 50 mL of acetonitrile, copper powder (0.35 g, 5.5 mmol) was added, and the mixture was stirred under argon at room temperature for 5 h. Excess copper was removed by filtration, and the purple filtrate was evaporated to give the product. Isolated in this way, the complex is obtained as an amorphous material; no solvent could be found to promote crystallization. The product was identified as $\text{Cu}(\text{PPh}_3)_2(3,5\text{-DBSQ})$ by its characteristic EPR spectrum.

$[\text{Cu}(\text{NCCH}_3)(\text{PPh}_3)]_2[\text{Cu}(3,5\text{-DBCat})_2]$. 3,5-DBBQ (1.1 g, 5.0 mmol) and PPh_3 (2.63 g, 10 mmol) were dissolved in acetonitrile (20 mL), copper powder (0.64 g, 10 mmol) was added, and the mixture was stirred under argon at reflux for 20 h. A brown powder deposited slowly during the course of the reaction. It was separated from the solution by filtration, washed with acetonitrile, and dried in vacuum. The copper complex was extracted with dichloromethane, and the volume of the solution was reduced to 50 mL under vacuum. Addition of ether (50 mL) gave $[\text{Cu}(\text{NCCH}_3)(\text{PPh}_3)]_2[\text{Cu}(3,5\text{-DBCat})_2]$ (2.8 g, 64% yield) as a bright brown powder. Anal. Calcd for $\text{C}_{68}\text{H}_{76}\text{N}_2\text{O}_4\text{P}_2\text{Cu}_3$: C, 65.97; H, 6.19; N, 2.26. Found: C, 65.24; H, 5.45; N, 2.1.

Physical Measurements. Electronic spectra were recorded on a Shimadzu UV-160A spectrophotometer, and infrared spectra were obtained on a Specord M-40 spectrometer (Carl Zeiss, Jena, Switzerland) with samples prepared as Nujol mulls. EPR spectra were recorded on a JEOL JES-FE/3X spectrometer, and magnetic measurements were made on a Quantum Design MPMS-5 SQUID magnetometer.

Crystallographic Structure Determinations. $[\text{Cu}(\text{py})_2(3,5\text{-DBCat})]_2$. Crystals obtained by slow evaporation of a pyridine solution formed as dark green-brown plates. Axial photographs indicated triclinic symmetry, and the centered settings of 25 reflections gave the unit cell dimensions listed in Table 1. Data were collected by θ - 2θ scans on a Siemens P3 diffractometer within the angular range 3.0–112.2°. The space group was assumed to be $P\bar{1}$, and the structure was solved using Patterson methods. The crystal structure consists of two independent $[\text{Cu}(\text{py})_2(3,5\text{-DBCat})]_2$ dimers located about crystallographic inversion centers at $[0, 0, 0]$ and $[0, 0, 1/2]$. One *tert*-butyl group of each dimer was rotationally disordered; they were refined with half methyl carbon atoms in staggered 3-fold positions with half-occupancy factors. A pyridine solvate molecule was found to be located near the inversion center at $[1/2, 1/2, 1/2]$. Atoms of this molecule were also refined with half-occupancies. Final cycles of refinement, including fixed contributions for the hydrogen atoms, converged with discrepancy indices of $R = 0.053$ and $R_w = 0.065$.

Table 2. Selected Atomic Coordinates ($\times 10^4$) for $[\text{Cu}(\text{py})_2(3,5\text{-DBCat})]_2$

	<i>x/a</i>	<i>y/b</i>	<i>z/c</i>	<i>U</i> (eq)
	Molecule 1			
Cu1	1136(1)	34(1)	4665(1)	45(1)
O1	-104(2)	819(2)	4435(2)	49(1)
O2	1775(2)	1217(2)	4004(2)	51(1)
N1	2258(2)	-540(2)	5330(2)	48(1)
N2	1781(2)	-682(2)	3330(2)	57(1)
C1	62(3)	1778(2)	4130(2)	40(1)
C2	1091(3)	1980(2)	3870(2)	43(1)
C3	1325(3)	2954(2)	3506(2)	48(1)
C4	525(3)	3682(3)	3461(2)	51(1)
C5	-494(3)	3508(3)	3740(2)	49(1)
C6	-704(3)	2528(2)	4077(2)	47(1)
C7	2429(3)	3194(3)	3150(3)	65(2)
C11	-1338(3)	4330(3)	3709(3)	65(2)
C15	3226(3)	-528(3)	4810(3)	66(2)
C16	3998(3)	-899(4)	5230(3)	80(2)
C17	3783(3)	-1298(4)	6228(3)	76(2)
C18	2790(3)	-1282(3)	6761(3)	65(2)
C19	2053(3)	-910(3)	6298(2)	53(1)
C20	1660(3)	-94(3)	2490(3)	73(2)
C21	2116(4)	-342(4)	1572(3)	77(2)
C22	2680(3)	-1196(4)	1529(3)	71(2)
C23	2827(4)	-1785(3)	2388(3)	79(2)
C24	2361(3)	-1511(3)	3267(3)	67(2)
	Molecule 2			
Cu2	-651(1)	-838(1)	458(1)	38(1)
O3	-693(2)	560(2)	427(2)	44(1)
O4	-2081(2)	-660(2)	1011(2)	44(1)
N3	-741(2)	-2031(2)	-27(2)	44(1)
N4	-332(2)	-1631(2)	1906(2)	54(1)
C25	-1676(2)	964(2)	619(2)	36(1)
C26	-2409(2)	286(2)	960(2)	38(1)
C27	-3439(2)	638(2)	1216(2)	38(1)
C28	-3681(2)	1644(2)	1087(2)	43(1)
C29	-2968(2)	2333(2)	719(2)	42(1)
C30	-1947(2)	1960(2)	505(2)	42(1)
C31	-4251(3)	-97(3)	1640(3)	50(1)
C35	-3284(3)	3422(3)	553(3)	61(2)
C39	-1287(4)	-2747(3)	571(3)	74(2)
C40	-1418(5)	-3542(4)	256(4)	102(3)
C41	-961(5)	-3594(4)	-717(4)	96(3)
C42	-429(4)	-2842(3)	-1347(3)	74(2)
C43	-331(3)	-2087(3)	-970(3)	54(2)
C44	-962(3)	-1370(3)	2706(3)	72(2)
C45	-890(4)	-1807(4)	3641(3)	81(2)
C46	-160(4)	-2547(3)	3770(3)	75(2)
C47	502(3)	-2806(3)	2972(3)	74(2)
C48	374(3)	-2336(3)	2056(3)	67(2)

^a The equivalent isotropic *U* is defined as one-third the trace of the orthogonalized U_{ij} tensor ($\text{Å}^2 \times 10^3$).

Tables containing atom positions, anisotropic displacement parameters, hydrogen atom positions, bond lengths, and bond angles are available as supplementary material.

$[\text{Cu}(\text{NCCH}_3)(\text{PPh}_3)]_2[\text{Cu}(3,5\text{-DBCat})_2]$. Crystals suitable for crystallographic analysis were obtained from the mother liquor as dark brown prisms. Axial photographs indicated monoclinic symmetry, and the centered settings of 25 reflections gave the unit cell dimensions listed in Table 1. Data were collected by θ - 2θ scans on a Siemens P3 diffractometer within the angular range 3.0–45.0°. The space group was found to be $P2_1/n$, and the structure was solved using Patterson methods. Final cycles of refinement, including fixed contributions for the hydrogen atoms, converged with discrepancy indices of $R = 0.037$ and $R_w = 0.056$. Tables containing atom positions, anisotropic displacement parameters, hydrogen atom positions, bond lengths, and bond angles are available as supplementary material.

Results

$[\text{Cu}(\text{py})_2(3,5\text{-DBCat})]_2$. Crystallographic characterization of $[\text{Cu}(\text{py})_2(3,5\text{-DBCat})]_2$ isolated from a pyridine solution shows that the molecule is dimeric. Selected atom locations are given in Table 2. The view of the molecule given in Figure 1 shows the square pyramidal coordination geometry about the metal ions,

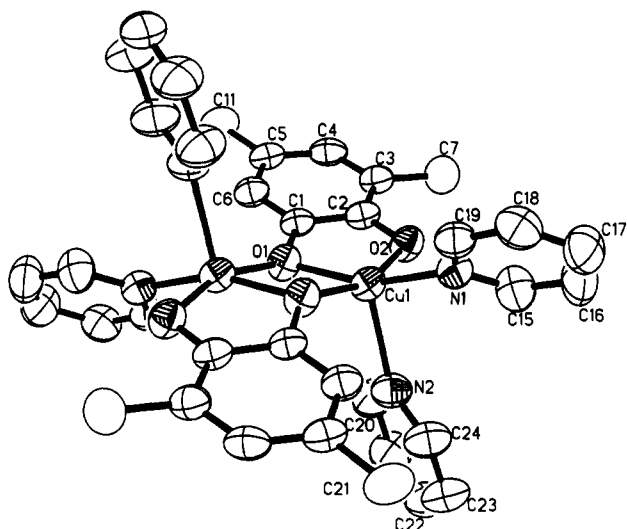


Figure 1. View of the $[\text{Cu}(\text{py})_2(3,5\text{-DBCat})]_2$ dimer.

Table 3. Selected Bond Lengths (Å) and Angles (deg) for $[\text{Cu}(\text{py})_2(3,5\text{-DBCat})]_2$

Molecule 1			
Bond Lengths			
Cu1-O1	1.964(2)	Cu1-O2	1.919(2)
Cu1-N1	2.034(3)	Cu1-N2	2.297(3)
Cu1-Cu1'	3.021(1)	Cu1-O1'	1.966(2)
O1-C1	1.354(4)	O2-C2	1.335(4)
Bond Angles			
O1-Cu1-O2	84.8(1)	O1-Cu1-N1	159.1(1)
O2-Cu1-N1	92.7(1)	O1-Cu1-N2	104.3(1)
O2-Cu1-N2	93.9(1)	N1-Cu1-N2	96.6(1)
Cu1-O1-Cu1'	100.5(1)		
Molecule 2			
Bond Lengths			
Cu2-O3	1.964(2)	Cu2-O4	1.908(2)
Cu2-N3	2.028(3)	Cu2-N4	2.260(3)
Cu2-Cu2'	3.008(1)	Cu2-O3'	1.958(2)
O3-C25	1.367(3)	O4-C26	1.336(4)
Bond Angles			
O3-Cu2-O4	84.7(1)	O3-Cu2-N3	157.0(1)
O4-Cu2-N3	92.9(1)	O3-Cu2-N4	105.2(1)
O4-Cu2-N4	94.5(1)	N3-Cu2-N4	97.8(1)
Cu2-O3-Cu2'	100.2(1)		

with pyridine ligands occupying apical sites. Basal coordination sites are occupied by the second pyridine ligand, oxygen atoms of a chelated catechololate ligand, and the catechololate oxygen of the ligand chelated to the adjacent metal. The link between adjacent metal ions is formed by the bridging catechololate oxygen atoms at basal coordination sites of both metals. Bond distances and angles given in Table 3 show that the Cu-O lengths for bridging and chelated bonds are essentially the same, 1.963(2) Å, and longer than the length to the terminal oxygen, 1.914(2) Å. The Cu-Cu' separations for the two unique dimers average to 3.015(1) Å. Bond lengths to the basal and apical pyridine ligands are significantly different, with the average basal length shorter at 2.031(3) Å than the apical length of 2.279(3) Å. Catechololate C-O bond lengths are typically longer for bonds to oxygen atoms that bridge metal ions, and this pattern appears for the $[\text{Cu}(\text{py})_2(3,5\text{-DBCat})]_2$ dimer. The average length to the bridging oxygens is 1.361(4) Å, while a length of 1.335(4) Å is found for the terminal oxygen atoms.

Spin density for the two $S = 1/2$ metal ions is concentrated in the metal $d\sigma$ orbital of the basal plane. EPR spectroscopy of the complex at room temperature in pyridine solution shows an isotropic spectrum centered about a g value of 2.111, with copper hyperfine coupling of 83.3 G. In the solid state the complex is

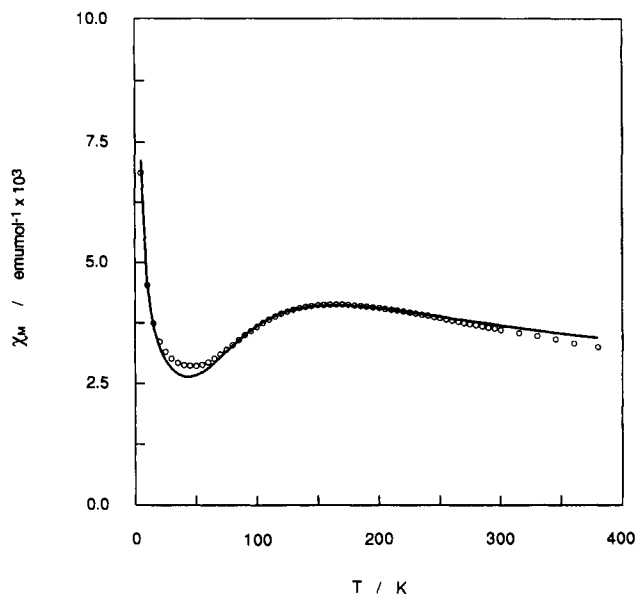


Figure 2. Plots of experimental (o) and calculated (—) values of magnetic susceptibility vs T for the $[\text{Cu}(\text{py})_2(3,5\text{-DBCat})]_2$ dimer.

EPR silent, but magnetic measurements show evidence for antiferromagnetic exchange between metal ions. At room temperature the magnetic moment, corrected for diamagnetic effects, is $2.84 \mu_B/\text{dimer}$, near the value for noninteracting spin centers. At 155 K evidence for exchange appears with a slight decrease to $2.29 \mu_B$, and the decrease in magnetic moment continues to a value of $0.52 \mu_B/\text{dimer}$ at 5.0 K. A plot of magnetic susceptibility versus temperature is shown in Figure 2 for $[\text{Cu}(\text{py})_2(3,5\text{-DBCat})]_2$ with the results of a theoretical fit for a J value of -95.3 cm^{-1} .¹⁰ The model used for exchange included a correction for the presence of a small quantity of paramagnetic impurity responsible for the "Curie tail" that appears at low temperature. Hatfield has correlated values for $2J$ with the Cu-O-Cu' bridge angle for a series of planar hydroxo-bridged dimers.¹¹ In particular, $[\text{Cu}(\text{dmaep})\text{OH}]_2^{2+}$ has a bridge angle of $100.4(1)^\circ$ and a $2J$ value of -200 cm^{-1} , in accord with prediction. The average Cu-O-Cu' bridge angle for $[\text{Cu}(\text{py})_2(3,5\text{-DBCat})]_2$ is $100.4(1)^\circ$ and the $2J$ value obtained from the theoretical model is close to the value anticipated from the Hatfield model, illustrating the aryloxo character of the catechololate bridge.

$[\text{Cu}(\text{NCCH}_3)(\text{PPh}_3)]_2[\text{Cu}(3,5\text{-DBCat})_2]$. The reaction between metallic copper and 3,5-DBBQ carried out in acetonitrile with 2 equiv of PPh_3 has been found to be dependent upon reaction conditions. Under mild conditions at room temperature, the product obtained shows the characteristic radical-based EPR signal of $\text{Cu}(\text{PPh}_3)_2(3,5\text{-DBSQ})$.¹² The spectrum is centered about a g value of 2.0047 and has been analyzed in terms of a hyperfine coupling pattern with $A(^{63}\text{Cu}) = 10.57 \text{ G}$, $A(^{65}\text{Cu}) = 11.32 \text{ G}$, $A(2\text{P}) = 16.00 \text{ G}$, $A(\text{H4}) = 3.18 \text{ G}$, and $A(\text{H}_{\text{r-Bu5}}) = 0.25 \text{ G}$. If the reaction is carried out with a second equivalent of copper metal under conditions of extended reflux, the product obtained gives the anisotropic copper-based EPR spectrum shown

- (10) Magnetic data for $[\text{Cu}(\text{py})_2(3,5\text{-DBCat})]_2$ were fit to the Bleaney-Bowers equation using the isotropic (Heisenberg) exchange Hamiltonian for two interacting $S = 1/2$ centers:

$$\chi_M = \frac{2N\beta^2 g^2}{kT} [3 + \exp(-2J/kT)]^{-1} (1 - P) + P \left[\frac{N\beta^2 g^2}{4kT} \right] + N\alpha$$

$$H = -2JS_1 S_2$$

A nonlinear regression analysis was used to give the best fit shown in Figure 2 for $J = -95.3 \text{ cm}^{-1}$, $g = 2.00$, and $P = 0.07$. Parameter P corrects for the presence of monomeric impurity.

- (11) Crawford, V. H.; Richardson, H. W.; Wasson, J. R.; Hodgson, D. J.; Hatfield, W. E. *Inorg. Chem.* 1976, 15, 2107.
 (12) Razuvaev, G. A.; Cherkasov, V. K.; Abakumov, G. A. *J. Organomet. Chem.* 1978, 160, 361.

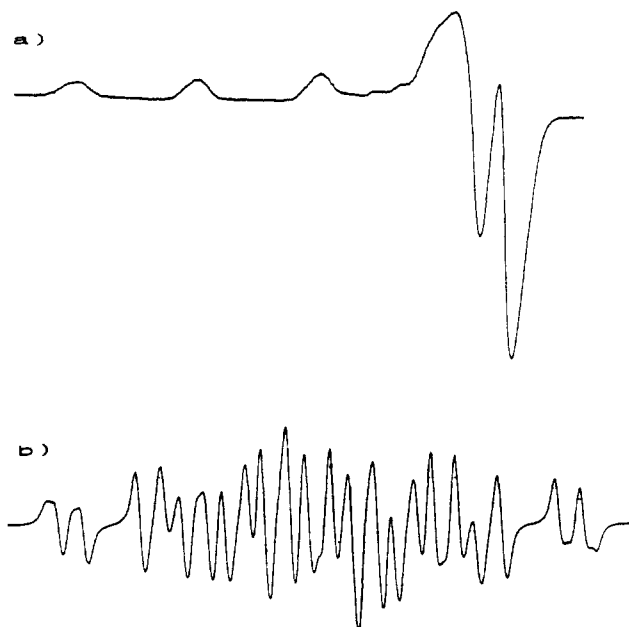


Figure 3. (a) EPR spectrum of $[\text{Cu}(\text{NCCH}_3)(\text{PPh}_3)_2][\text{Cu}(3,5\text{-DBCat})_2]$ recorded on a solid sample at room temperature. Parameters: $g_{\perp} = 2.253$; $g_{\parallel} = 2.060$; $A_{\perp} = 167.5 \text{ G}$ (^{63}Cu), 180.0 G (^{65}Cu); $A_{\parallel} = 20 \text{ G}$. (b) EPR spectrum of $(\text{PPh}_3)_2\text{Cu}(3,5\text{-DBSQ})$ and of $[\text{Cu}(\text{PPh}_3)(\text{NCCH}_3)]_2[\text{Cu}(3,5\text{-DBCat})_2]$ in toluene solution at room temperature. Parameters: $g = 2.0047$; $A(^{63}\text{Cu}) = 10.57 \text{ G}$; $A(^{65}\text{Cu}) = 11.32 \text{ G}$; $A(2\text{P}) = 16.00 \text{ G}$; $A(\text{H}4) = 3.18 \text{ G}$; $A(\text{Bu}5) = 0.25 \text{ G}$.

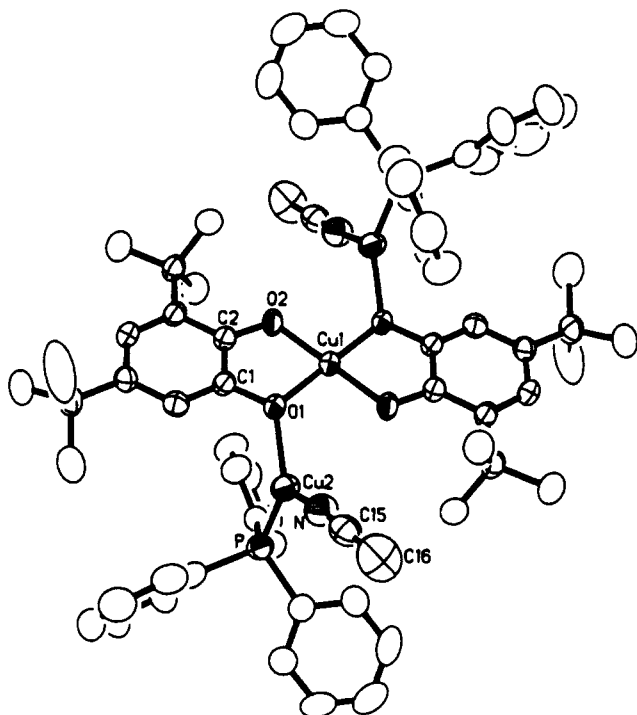


Figure 4. View of $[\text{Cu}(\text{NCCH}_3)(\text{PPh}_3)_2][\text{Cu}(3,5\text{-DBCat})_2]$.

in Figure 3. Structural characterization of the complex has shown that it consists of a planar $\text{Cu}^{\text{II}}(3,5\text{-DBCat})_2^{2-}$ core with $\text{Cu}^{\text{I}}(\text{NCCH}_3)(\text{PPh}_3)^+$ cations bound to bridging catecholate oxygens of the anion. A view of the molecule is shown in Figure 4, selected atomic coordinates are given in Table 4, and bond lengths and angles are listed in Table 5. The central $\text{Cu}(\text{II})$ ion is located at a crystallographic inversion center, requiring that the $\text{Cu}(3,5\text{-DBCat})_2^{2-}$ anion be rigorously planar. Cationic $\text{Cu}^{\text{I}}(\text{NCCH}_3)(\text{PPh}_3)^+$ fragments are bound to the oxygen atom at the C1 ring position on either side of the plane with $\text{Cu}1\text{-O}1\text{-Cu}2$ bond angles of $118.2(1)^\circ$. Bond angles about Cu2 show

Table 4. Selected Atomic Coordinates ($\times 10^4$) for $[\text{Cu}(\text{NCCH}_3)(\text{PPh}_3)_2][\text{Cu}(3,5\text{-DBCat})_2]$

	x/a	y/b	z/c	$U(\text{eq})^a$
Cu1 ^b	0	0	0	36(1)
Cu2	-176(1)	2315(1)	1170(1)	47(1)
P	-33(1)	1626(1)	2159(1)	45(1)
O1	-697(2)	1266(3)	406(1)	40(1)
O2	-931(2)	-1268(3)	-139(1)	42(1)
C1	-1490(2)	697(4)	349(2)	34(1)
C2	-1599(2)	-665(4)	57(2)	35(1)
C3	-2400(2)	-1326(4)	-6(2)	36(1)
C4	-3037(2)	-557(4)	216(2)	38(1)
C5	-2927(2)	800(4)	497(2)	38(1)
C6	-2128(2)	1408(4)	560(2)	40(1)
N	164(3)	4224(4)	922(2)	57(1)
C15	438(3)	5340(5)	855(2)	55(2)
C16	808(5)	6752(5)	768(3)	98(3)
C17	-902(3)	2138(5)	2548(2)	51(2)
C23	26(3)	-337(5)	2271(2)	43(1)
C29	884(3)	2370(5)	2681(2)	49(2)

^a The equivalent isotropic U is defined as one-third the trace of the orthogonalized U_{ij} tensor ($\text{\AA}^2 \times 10^3$). ^b Refined with an occupancy factor of 0.5.

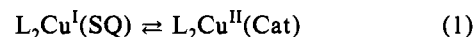
Table 5. Selected Bond Lengths (\AA) and Angles (deg) for $[\text{Cu}(\text{NCCH}_3)(\text{PPh}_3)_2][\text{Cu}(3,5\text{-DBCat})_2]$

Bond Lengths			
Cu1-O1	1.929(3)	Cu1-O2	1.891(2)
Cu2-P	2.176(1)	Cu2-O1	1.957(2)
Cu2-N	1.948(4)	O1-C1	1.371(4)
O2-C2	1.343(5)	N-C15	1.142(6)
Bond Angles			
O1-Cu1-O2	86.4(1)	O1-Cu1-O2'	93.6(1)
P-Cu2-O1	128.3(1)	P-Cu2-N	122.6(1)
O1-Cu2-N	109.0(1)	Cu1-O1-Cu2	118.2(1)
Cu1-O1-C1	109.6(2)	Cu2-O1-C1	121.8(2)
Cu1-O2-C2	110.7(2)	Cu2-N-C15	170.6(4)

that the coordination geometry is triangular planar. The magnetic moment measured for the complex at room temperature is $1.97 \mu_{\text{B}}$, and the central $\text{Cu}(\text{II})$ ion is the paramagnetic center. The EPR spectrum shown in Figure 3 was recorded on a solid sample of the complex; spectra recorded in solution show a shift to a radical-based magnetic center. Indeed, the spectrum obtained for $[\text{Cu}(\text{NCCH}_3)(\text{PPh}_3)_2][\text{Cu}(3,5\text{-DBCat})_2]$ in toluene solution is identical with the characteristic spectrum of $(\text{PPh}_3)_2\text{Cu}^{\text{I}}(3,5\text{-DBSQ})$ shown in Figure 3.

Discussion

Charge distribution within the metal-quinone chelate ring is sensitive to the orbital energy of the metal ion. For complexes of copper, coligand bonding effects may be used to direct charge distribution with accompanying changes in magnetic properties and stereochemistry. Prior studies have shown that, with phosphine, CO, olefin, and alkyne coligands, the $\text{L}_2\text{Cu}^{\text{I}}(\text{SQ})$ charge distribution is obtained and complexes of this form generally exhibit characteristic radical-based EPR spectra.^{12,13} With nitrogen-donor coligands, the $\text{L}_2\text{Cu}^{\text{II}}(\text{Cat})$ charge distribution results and the paramagnetic center shifts to the metal.^{8,14} With an appropriate choice of coligand, the balance of metal and quinone orbital energies may be such that an equilibrium between $\text{Cu}^{\text{I}}(\text{SQ})$ and $\text{Cu}^{\text{II}}(\text{Cat})$ species may be observed:



Redox equilibria of this type are known for complexes of cobalt

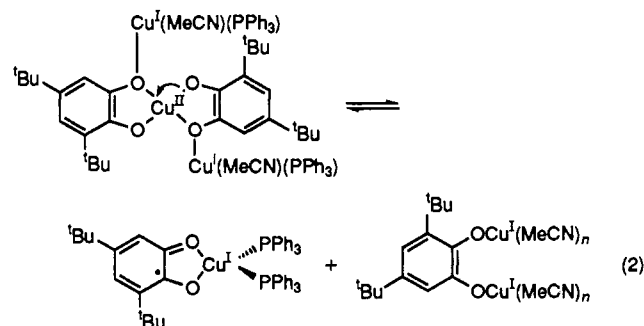
- (13) Kashtanov, E. A.; Cherkasov, V. K.; Gorbunova, L. V.; Abakumov, G. A. *Izv. Akad. Nauk SSSR, Ser. Khim.* **1983**, 2121.
 (14) Abakumov, G. A.; Cherkasov, V. K.; Lobanov, A. V. *Dokl. Akad. Nauk SSSR* **1982**, 266, 361.

and manganese,¹⁵ and spectroscopic changes observed in solution for complexes of Ni, Rh, and Ir have been interpreted as indicating similar equilibria involving metal–quinone electron transfer.¹⁶

Coligand bonding effects and the choice of quinone ligand combine to define charge distribution. The copper complex of 9,10-phenanthrenequinone containing pyridine coligands appears to have the Cu^I charge distribution, (py)₂Cu^I(PhenSQ), while with the 3,5-DBBQ ligand the complex contains Cu^{II}.² Structurally, [Cu(py)₂(3,5-DBCat)]₂ differs from the 2,2'-bipyridine analog in the nature of the bridging interaction, and this contributes to differences in the magnetic properties of the two complexes. The metal centers of [(bpy)Cu(3,5-DBCat)]₂ also have square pyramidal coordination geometries, but planar complex units stack atop one another and the bridging interactions between catecholate oxygens and the adjacent metals are between basal and apical coordination sites.⁸ The Cu–Cu' separation is 3.074 Å, slightly longer than the value for the bis(pyridine) dimer, and the Cu–O–Cu' angle for the bridge is 92.5°. Orthogonality of the magnetic planes of the complex units of [Cu(bpy)(3,5-DBCat)]₂ results in a far weaker exchange interaction than that observed for [Cu(py)₂(3,5-DBCat)]₂ despite their similarity in composition.

Equilibria of the type described in eq 1 may be observed as temperature-dependent changes in EPR spectra. Differences in the preferred stereochemistry of Cu(I) and Cu(II) may introduce a significant barrier to metal–quinone electron transfer as a shift between tetrahedral and planar geometries may accompany changes in metal oxidation state. Such an equilibrium has been reported for a complex containing the 3,6-DBQ ligand and a 1,4-diazabutadiene coligand on the basis of reversible changes in the EPR spectrum.¹⁷ Structural characterization of a form of the complex prepared with 1,4-di-*tert*-butyl-1,4-diazabutadiene and 3,6-di-*tert*-butyl-4-chloro-1,2-benzoquinone showed separate

[Cu^I(Bu₂aza)₂]⁺ cations and [Cu(SQ)(Cat)]⁻ anions, however.¹⁸ The change in the EPR spectrum of Cu^I(PPh₃)₂(3,5-DBSQ) in acetonitrile solution from a radical-based spectrum to one of Cu(II) is associated with formation of [Cu(NCCH₃)(PPh₃)₂][Cu(3,5-DBCat)₂]. The reappearance of the spectrum of Cu^I(PPh₃)₂(3,5-DBSQ) upon dissolving a solid sample of [Cu(NCCH₃)(PPh₃)₂][Cu(3,5-DBCat)₂] in toluene is surprising but can be explained in terms of a reaction that involves back electron transfer within the [Cu(3,5-DBCat)₂]²⁻ unit of [Cu(NCCH₃)(PPh₃)₂][Cu(3,5-DBCat)₂] shown in eq 2. Studies on quantitative



aspects of this reaction and the dependence of electron transfer on solvent polarity are continuing.

Acknowledgment. We thank Brenda Conklin for recording variable-temperature magnetic measurements and Dr. Antal Rockenbauer for obtaining EPR spectra. Support for research carried out at the University of Colorado was provided by the National Science Foundation (Grant CHE 90-23636). Research at the University of Veszprem was supported by the Hungarian Research Fund (Grant OTKA-2326). C.G.P. and G.S. thank the U.S.-Hungarian Joint Fund for collaborative research support through Grant 098/91.

Supplementary Material Available: Tables giving crystal data and details of the structure determination, atomic coordinates, anisotropic thermal parameters, hydrogen atom locations, and bond lengths and angles for [Cu(py)₂(3,5-DBCat)]₂ and [Cu(NCCH₃)(PPh₃)₂][Cu(3,5-DBCat)₂] (27 pages). Ordering information is given on any current masthead page.

- (15) (a) Buchanan, R. M.; Pierpont, C. G. *J. Am. Chem. Soc.* **1980**, *102*, 4951. (b) Lynch, M. W.; Hendrickson, D. N.; Fitzgerald, B. J.; Pierpont, C. G. *J. Am. Chem. Soc.* **1984**, *106*, 2041.
- (16) (a) Abakumov, G. A.; Razuvaev, G. A.; Nevodchikov, V. I.; Cherkasov, V. K. *J. Organomet. Chem.* **1988**, *341*, 485. (b) Rakhimov, R. R.; Solozhenkin, P. M.; Kopitaya, N. N.; Pupkov, V. S.; Prokofev, A. I. *Dokl. Akad. Nauk SSSR* **1988**, *300*, 1177. (c) Abakumov, G. A.; Garnov, V. A.; Nevodchikov, V. I.; Cherkasov, V. K. *Dokl. Akad. Nauk SSSR* **1989**, *304*, 107.
- (17) (a) Abakumov, G. A.; Garnov, V. A.; Nevodchikov, V. I.; Cherkasov, V. K. *Dokl. Akad. Nauk SSSR* **1989**, *304*, 107. (b) Abakumov, G. A.; Cherkasov, V. K. *Metallorg. Khim.* **1990**, *3*, 838.

- (18) Zakharov, L. N.; Saf'yanov, Yu. N.; Struchkov, Yu. T.; Abakumov, G. A.; Cherkasov, V. K.; Garnov, V. A. *Koord. Khim.* **1990**, *16*, 802.